



## Artificial Humming Bird Optimization with Siamese Convolutional Neural Network Based Fruit Classification Model

T. Satyanarayana Murthy<sup>1</sup>, Kollati Vijaya Kumar<sup>2</sup>, Fayadh Alenezi<sup>3</sup>, E. Laxmi Lydia<sup>4</sup>, Gi-Cheon Park<sup>5</sup>, Hyoung-Kyu Song<sup>6</sup>, Gyanendra Prasad Joshi<sup>7</sup> and Hyeonjoon Moon<sup>7,\*</sup>

<sup>1</sup>Department of Information Technology, Chaitanya Bharathi Institute of Technology, Hyderabad, Telangana, India

<sup>2</sup>Department of Computer Science, College of Computer and Information Sciences, Majmaah University, Al-Majmaah, 11952, Saudi Arabia

<sup>3</sup>Department of Electrical Engineering, College of Engineering, Jouf University, Sakaka, Saudi Arabia

<sup>4</sup>Department of Computer Science and Engineering, Vignan's Institute of Information Technology, Visakhapatnam, 530049, India

<sup>5</sup>Department of International Affairs and Education, Gangseo University, Seoul, 07661, Korea

<sup>6</sup>Department of Information and Communication Engineering and Convergence Engineering for Intelligent Drone, Sejong University, Seoul, 05006, Korea

<sup>7</sup>Department of Computer Science and Engineering, Sejong University, Seoul, 05006, Korea

\*Corresponding Author: Hyeonjoon Moon. Email: hmoon@sejong.ac.kr

Received: 27 July 2022; Accepted: 26 October 2022; Published: 28 July 2023

**Abstract:** Fruit classification utilizing a deep convolutional neural network (CNN) is the most promising application in personal computer vision (CV). Profound learning-related characterization made it possible to recognize fruits from pictures. But, due to the similarity and complexity, fruit recognition becomes an issue for the stacked fruits on a weighing scale. Recently, Machine Learning (ML) methods have been used in fruit farming and agriculture and brought great convenience to human life. An automated system related to ML could perform the fruit classifier and sorting tasks previously managed by human experts. CNN's (convolutional neural networks) have attained incredible outcomes in image classifiers in several domains. Considering the success of transfer learning and CNNs in other image classifier issues, this study introduces an Artificial Humming Bird Optimization with Siamese Convolutional Neural Network based Fruit Classification (AMO-SCNNFC) model. In the presented AMO-SCNNFC technique, image preprocessing is performed to enhance the contrast level of the image. In addition, spiral optimization (SPO) with the VGG-16 model is utilized to derive feature vectors. For fruit classification, AHO with end to end SCNN (ESCNN) model is applied to identify different classes of fruits. The performance validation of the AMO-SCNNFC technique is tested using a dataset comprising diverse classes of fruit images. Extensive comparison studies reported improving the AMO-SCNNFC technique over other approaches with higher accuracy of 99.88%.

**Keywords:** Fruit classification; computer vision; machine learning; deep learning; metaheuristics



## 1 Introduction

Automated fruit classification is an exciting challenge in developing fruit and retailing industrial chains as it is useful for supermarkets and fruit producers to discover several fruits and their condition from the stock or container to improvise production and income of the business [1]. Therefore, intellectual mechanisms with computer vision (CV) and machine learning (ML) techniques were implemented for classification, fruit defect recognition, and ripeness grading for the past few decades in automated fruit classifications, 2 main approaches, deep learning (DL)-based methods and conventional CV-related methods are inspected [2]. The conventional CV-based approaches initially extract the lower-level features. They do image classifiers via the conventional ML techniques, whereas the DL-based approaches effectively extract the features and implement an end-wise image classification [3]. In CV techniques and conventional image processing, image features, colour, shape, and texture are input units for fruit classifiers [4]. Former, fruit processing and selection rely on artificial approaches, resulting in a vast volume of waste of labor [5]. With the rapid development of 4G communication and wide familiarity with numerous mobile Internet devices, people have constituted many images, videos, sounds, and other data, and image-identifying technology has gradually matured [6]. Image-based fruit recognition has grabbed the author's interest due to its low-cost devices and incredible performances. Meanwhile, it has to devise automated tools to deal with unplanned situations like an accidental mixture of fresh goods, placement of fruit in unusual packaging, spider webs on the lens, various lighting conditions, and so on [7]. DL refers to a subfield of ML which has shown outstanding outcomes in image detection [8]. DL uses the multilayer structure for processing image features that pointedly raise the efficiency of image recognition. Otherwise, implementing image detection and DL becomes a concept in the supply chain and logistics [9]. Another application of DL is the fruit classifier. DL could efficiently derive image features after the present classification [10]. Current CV advancements have shown outstanding fallouts in many areas of life. Fruit classification and detection have been illustrated as complicated and challenging tasks.

Chen et al. [11] devise a fruit image classifier algorithm related to the multi-optimization CNN with the background of the fruit classifier. Initially, to avoid the interference of exterior noise and influences on the classifier accurateness, the wavelet thresholds can be employed to denoise the fruit image, that could diminish image noises while preserving the image details. Then, the gamma transformation can be applied for image correction to rectify the over-dark fruit image or over-bright fruit image. At last, in the process of building the CNN, the SOM network can be presented for pre-learning the samples. Ashraf et al. [12] formulate a mechanism trained with a fruit image data set and identifies whether the fruit is fresh or rotten from an input image. And framed the initial method utilizing the Inception V3 algorithm and trained with this dataset implementing TL.

In [13], the authors designed a new fruit classifier algorithm using Recurrent Neural Network (RNN) architectures, CNN features, and LSTM. Type-II fuzzy enhancement was even utilized as a pre-processor tool for enhancing the images. Moreover, to fine-tune the hyperparameters of the devised method, TLBO-MCET was employed. Shahi et al. [14] project a lightweight DL technique utilizing the attention module and pretrained MobileNetV2 method. Firstly, the convolution features were derived for capturing high-level object-related data. Secondly, an attention module was employed to capture the exciting semantic data. The convolution and attention modules were compiled together to merge the interesting semantic information and high-level object-related data that can be pursued by the softmax-and FC layers.

Zhu et al. [15] devised a high-performance approach for vegetable images classifier related to DL structure. The AlexNet network method in Caffe has been leveraged for training the vegetable image dataset. The vegetable image dataset has been acquired from ImageNet and classified into a test dataset and training dataset. The output functioning of the AlexNet network implemented the Rectified Linear Units (ReLU) rather than the conventional tanh function and sigmoid function that hastened the training of the DL network. The dropout technology has been utilized for enhancing model generalization. In [16], this crew formulated a 13-layer CNN. Three kinds of data augmenting approaches are employed:

noise injection, image rotation, and Gamma correction. And comparison was made between average pooling with max pooling. The stochastic gradient descent (SGD) with momentum has been utilized for training the CNN with a minibatch size of 128. Though several models are available in the literature, there is still a room to improve the classification performance. Most of the existing works have not focused on hyperparameter tuning process, which is addressed in this work.

This study introduces an Artificial Humming Bird Optimization with Siamese Convolutional Neural Network based Fruit Classification (AMO-SCNNFC) model. In the presented AMO-SCNNFC technique, image preprocessing is performed to enhance the contrast level of the image. In addition, spiral optimization (SPO) with the VGG-16 model is utilized to derive feature vectors. For fruit classification, AHO with an end-to-end (ESCNN) model is applied to identify different classes of fruits. The performance validation of the AMO-SCNNFC technique is tested using a dataset comprising diverse classes of fruit images.

## 2 Materials and Methods

In this study, a new AMO-SCNNFC model has been developed for the automated classification of fruits. The AMO-SCNNFC technique encompasses preprocessing, VGG-16 feature extraction, SPO hyperparameter tuning, ESCNN classification, and AHO-based parameter optimization. Using SPO and AHO techniques helps accomplish enhanced fruit classification performance. Fig. 1 depicts the block diagram of the AMO-SCNNFC approach.

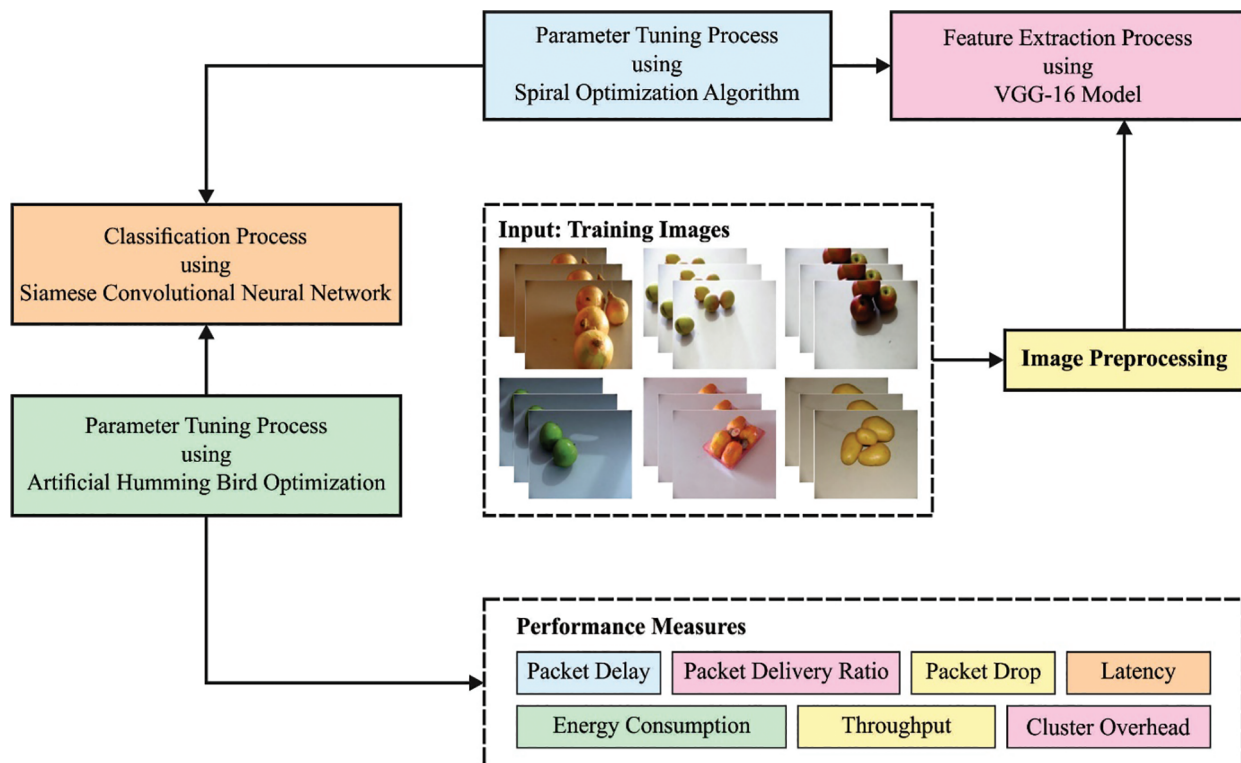


**Figure 1:** Block diagram of AMO-SCNNFC approach

### 2.1 Feature Extraction: VGG-16 Model

In this work, the input fruit images are given into the VGG-16 model to derive feature vectors. A CNN is the most effective kind of DL technique [17]. It employs a deep convolution network and non-linearity for



Now,  $i_\ell, j_\ell \in \{1, \dots, n\}$ ,  $i_\ell < j_\ell$ , ( $l = 1, \dots, 0$ ), and the blank element indicates 0. In Eq. (1) using  $R(\theta) = R_{1,2}(\theta)$ ,  $x^* = [55]^T$ ,  $x(O) = [1010]^T$  in  $2D$  space and  $R(\theta) = R_{2,3}(\theta)R_{1,3}(\theta)R_{1,2}(\theta)$ ,  $x^* = [505]^T$ ,  $x(O) = [151515]^T$  in  $3D$  space. In both cases, we observed the spiral trajectory produced nearby and the impact of the parameter.

The inspiration for the presented approach was the comprehension that the dynamic generating logarithmic spiral seems to have an affinity with the efficient technique of metaheuristics, “diversification in the initial half and intensification in the next half.

- Diversification: Search for good solutions by seeking a wider area.
- Intensification: Search for a good solution by seeking intensely nearby a better solution.

Subsequently, the SPO approach is a direct multi-point search technique that employs different general spiral mechanisms of Eq. (1) and is defined in case of a problem to minimize an objective function:  $\mathbb{R}^n \rightarrow \mathbb{R}(n \geq 2)$ :

Minimize  $f(x)$  as follows.  
 $x \in \mathbb{R}^n$

### 2.3 Fruit Classification: SCNN Model

For fruit classification, the ESCNN model is applied to identify different classes of fruits. An important development in the original SCNN to ESCNN is that ESCNN was provided with a fully connected (FC) network for replacing the energy function and resultant layer from the original SCNN [19]. The resultant layer of ESCNN comprises several neurons that allow it for managing multi-class classifier tasks directly. While the alteration of network topology, related to SCNN, ESCNN labeling approach of sample-pair, the process of creating classifier map and loss function were established as follows. It can be executing the labeling approach of the sample pair presented. Afterwards, labeling the sample-pair set by this approach, the labeled sample-pair set comprises another class than the original trained set. In detail, when the trained set involves  $C$  classes, the labeled sample-pair set comprises  $C + 1$  classes, and the extra class  $(C + 1)^{th}$  the label represents that these 2 instances of a sample pair do not go to several similar classes. While the input of ESCNN is a sample pair, it can execute a neighborhood voting approach for determining the class label of center pixels lastly. Fig. 2 illustrates the structure of SNN.

The underlying assumption of this approach is that the central pixel has a higher probability of going to a similar class as their neighbor pixels. Consider that a  $3 \times 3$  neighborhood was selected. Specifically, to a pixel, that classification can be initially chosen as a  $5 \times 5$  neighborhood of pixels for obtaining 24-pixel pairs. Afterward, it can supply these pixel pairs as a trained network for predicting its labels. To provide the predicted labels, it can be primary, excluding the pixel-pairs that don't concern a similar class; next, the label with a very important amount of votes is chosen as the center pixel class label. While the resultant of ESCNN comprises several neurons, it can be presented as a novel version of the cross-entropy loss function in Eqs. (3) and (4).

$$E = -\frac{1}{n} \sum_{i=1}^n \left\{ \sum_{k=1}^n [y_{ik} \log(\hat{y}_{ik})C + 1 + (1 - y_{ik}) \log(1 - \hat{y}_{ik})] + \alpha * Q_i \right\} \quad (3)$$

$$Q_j = \frac{1}{C} \sum_{j=1}^{C+1} y_{ij} \left[ \hat{y}_{ik} + \mu - \sum_{k=1}^{C+1} (y_{ik} \hat{y}_{ik}) \right]_+ \quad (4)$$

whereas  $n$  refers to the batch size,  $\mu$  signifies the decimal between zero and one. The term  $[z]_+ = \max(z, 0)$  signifies the standard hinge loss.  $y_i$  refers to the label of  $i^{th}$  pixel-pair, and  $(y_{i1}, \dots, y_{ik}, \dots, y_{i(C+1)})$  represents the one-hot label of  $y_j$ .  $y_j$  stands for the predictive value of  $i^{th}$  pixel-pair, and  $(y_{i1}, \dots, y_{ik}, \dots, y_{i(C+1)})$  represents the one-hot label of  $y_i$ .  $Q_i$  denotes the regularized for guaranteeing the accuracy of the HSI classifier.  $\alpha$  implies the weighted coefficient.

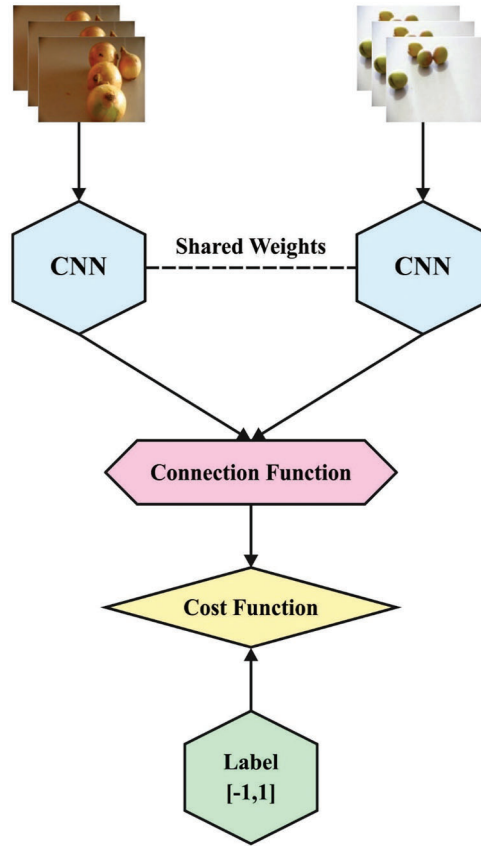


**Figure 2:** Structure of SNN

To adjust the hyperparameters related to the ESCNN model, the AHB is used. The AHB technique was employed to efficiently alter the parameters contained in the ESCNN technique to achieve maximal classifier efficiency [20]. The AHB technique is an optimized method inspired by the foraging and flight of hummingbirds. The 3 important processes are offered as follows: during the guided foraging method, 3 flight performances were employed from the foraging (omnidirectional, axial, and diagonal flights). It could be demonstrated as:

$$v_i(t+1) = x_{i,ta}(t) + h.b.(x_i(t) - X_{i,ta}(t))h \sim N(0, 1) \quad (5)$$

whereas  $x_{i,ta}(t)$  exemplifies the place of targeted food sources,  $h$  represents the guiding factor, and  $x(t)$  defines the place of  $i^{th}$  food source at time  $t$ . The place upgrading of  $i^{th}$  the food source was offered as:

$$x_{Ai}(t) = \begin{cases} x_i(t) & f(x_i(t)) \leq f(v_i(t+1)) \\ v_i(t+1) & f(x_i(t)) > f(v_i(t+1)) \end{cases} \quad (6)$$

In which  $f(x_i(t))$  and  $f(v_i(t+1))$  stands for the value of fitness functions for  $x(t)$  and  $v_i(t+1)$ . The local searching of hummingbirds from the territorial foraging approach was offered from the subsequent:

$$v_i(t+1) = x_{i(t)} + g.b.(\chi_{i(t)})g \sim N(0, 1) \quad (7)$$

whereas  $g$  implies the territorial feature. The arithmetical equation for migrating foraging of hummingbirds is offered as:

$$x_{wor}(t+1) = lb + r.(ub - lb) \quad (8)$$

In which  $x_{wor}$  specifies the food source with the worse rate of populations of the nectar refilling,  $r$  denotes the haphazard influence, and  $ub$  and  $lb$  demonstrate the upper as well as lower limits correspondingly.

The AHB algorithm makes derivations of a fitness function (FF) for achieving enhanced classifier outcomes. It sets a positive numeral for indicating the superior outcome of the candidate solutions. The reduction of the classifier error rate can be regarded as the FF, as presented in Eq. (9).

$$fitness(x_i) = Classifier\ Error\ Rate(x_i) = \frac{number\ of\ misclassified\ samples}{Total\ number\ of\ samples} * 100 \quad (9)$$

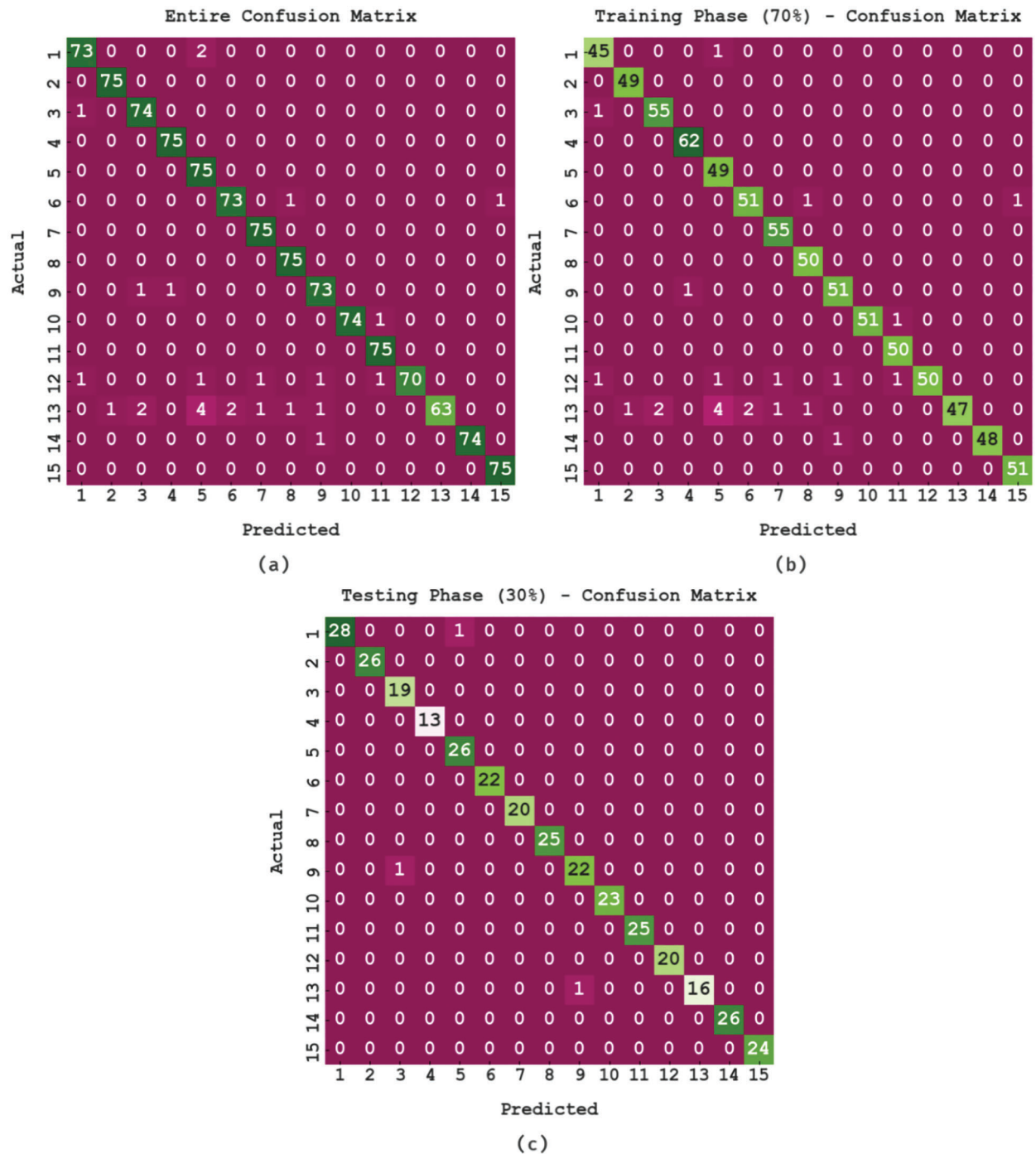
### 3 Results and Discussion

The proposed model is simulated using Python 3.6.5 tool on PC i5-8600k, GeForce 1050Ti 4 GB, 16 GB RAM, 250 GB SSD, and 1TB HDD. The parameter settings are given as follows: learning rate: 0.01, dropout: 0.5, batch size: 5, epoch count: 50, and activation: ReLU. This section inspects the fruit classification performance of the AMO-SCNNFC model on an openly accessible fruit and vegetable dataset [21] that comprises 15 classes as shown in Table 1. All the classes involve at least 75 images, resulting in 2633 images in total.

**Table 1:** Dataset details

Labels	Class	No. of samples
1	Agata potato	75
2	Asterix potato	75
3	Cashew	75
4	Diamond peach	75
5	Fuji apple	75
6	Granny smith apple	75
7	Honeydew melon	75
8	Kiwi	75
9	Nectarine	75
10	Onion	75
11	Orange	75
12	Plum	75
13	Spanish pear	75
14	Tahiti lime	75
15	Watermelon	75
<b>Total number of samples</b>		<b>1125</b>

Fig. 3 represents the confusion matrices produced by the AMO-SCNNFC model. The figure ensured that the AMO-SCNNFC model had effectually identified different kinds of fruit classes proficiently.



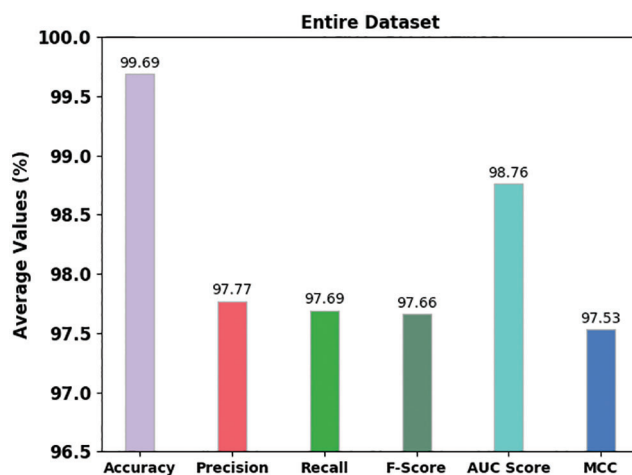
**Figure 3:** Confusion matrices of AMO-SCNNFC approach (a) Entire dataset, (b) 70% of TR data, and (c) 30% of TS data

Table 2 and Fig. 4 portrayed the fruit classification results of the AMO-SCNNFC model on the entire dataset. The AMO-SCNNFC method has classified samples under class 1 with  $accu_y$ ,  $prec_n$ ,  $reca_l$ ,  $F_{score}$ ,  $AUC_{score}$ , and MCC of 99.64%, 97.33%, 97.33%, 97.33%, 98.57%, and 97.14% respectively. At the same time, the AMO-SCNNFC algorithm has categorized samples under class 5 with  $accu_y$ ,  $prec_n$ ,  $reca_l$ ,  $F_{score}$ ,  $AUC_{score}$ , and MCC of 99.38%, 91.46%, 100%, 95.54%, 99.67%, and 93.52% correspondingly. Finally, the AMO-SCNNFC method has categorized samples under class 10 with  $accu_y$ ,  $prec_n$ ,  $reca_l$ ,  $F_{score}$ ,  $AUC_{score}$ , and MCC of 99.91%, 100%, 98.67%, 99.33%, 99.33%, and 99.28% correspondingly. Finally, the AMO-SCNNFC approach has categorized samples under class 15 with  $accu_y$ ,  $prec_n$ ,  $reca_l$ ,  $F_{score}$ ,  $AUC_{score}$ , and MCC of 99.91%, 98.68%, 100%, 99.34%, 99.95%, and 99.29% correspondingly.

**Table 2:** Result analysis of AMO-SCNNFC approach with distinct class labels under the entire dataset

Entire dataset						
Labels	Accuracy	Precision	Recall	F-score	AUC score	MCC
1	99.64	97.33	97.33	97.33	98.57	97.14
2	99.91	98.68	100.00	99.34	99.95	99.29
3	99.64	96.10	98.67	97.37	99.19	97.19
4	99.91	98.68	100.00	99.34	99.95	99.29
5	99.38	91.46	100.00	95.54	99.67	95.32
6	99.64	97.33	97.33	97.33	98.57	97.14
7	99.82	97.40	100.00	98.68	99.90	98.60
8	99.82	97.40	100.00	98.68	99.90	98.60
9	99.56	96.05	97.33	96.69	98.52	96.45
10	99.91	100.00	98.67	99.33	99.33	99.28
11	99.82	97.40	100.00	98.68	99.90	98.60
12	99.56	100.00	93.33	96.55	96.67	96.38
13	98.93	100.00	84.00	91.30	92.00	91.13
14	99.91	100.00	98.67	99.33	99.33	99.28
15	99.91	98.68	100.00	99.34	99.95	99.29
<b>Average</b>	<b>99.69</b>	<b>97.77</b>	<b>97.69</b>	<b>97.66</b>	<b>98.76</b>	<b>97.53</b>

Table 3 and Fig. 5 portrayed the fruit classification results of the AMO-SCNNFC model on 70% of training (TR) data. The AMO-SCNNFC algorithm has classified samples under class 1 with  $accu_y$ ,  $prec_n$ ,  $reca_l$ ,  $F_{score}$ ,  $AUC_{score}$ , and MCC of 99.62%, 95.74%, 97.83%, 96.77%, 98.78%, and 96.56% correspondingly. At the same time, the AMO-SCNNFC approach has categorized samples under class 5 with  $accu_y$ ,  $prec_n$ ,  $reca_l$ ,  $F_{score}$ ,  $AUC_{score}$ , and MCC of 99.24%, 89.09%, 100%, 94.23%, 99.59%, and 94% correspondingly. Ultimately, the AMO-SCNNFC technique has categorized samples under class 10 with  $accu_y$ ,  $prec_n$ ,  $reca_l$ ,  $F_{score}$ ,  $AUC_{score}$ , and MCC of 99.87%, 100%, 98.08%, 99.03%, 99.04%, and 98.97% correspondingly. Finally, the AMO-SCNNFC algorithm has categorized samples under class 15 with  $accu_y$ ,  $prec_n$ ,  $reca_l$ ,  $F_{score}$ ,  $AUC_{score}$ , and MCC of 99.87%, 98.08%, 100%, 99.03%, 99.93%, and 98.97% correspondingly.



**Figure 4:** Result analysis of AMO-SCNNFC approach under the entire dataset

**Table 3:** Result analysis of AMO-SCNNFC approach with distinct class labels under 70% of TR data

Training phase (70%)						
Labels	Accuracy	Precision	Recall	F-score	AUC score	MCC
1	99.62	95.74	97.83	96.77	98.78	96.58
2	99.87	98.00	100.00	98.99	99.93	98.93
3	99.62	96.49	98.21	97.35	98.97	97.14
4	99.87	98.41	100.00	99.20	99.93	99.13
5	99.24	89.09	100.00	94.23	99.59	94.00
6	99.49	96.23	96.23	96.23	97.98	95.95
7	99.75	96.49	100.00	98.21	99.86	98.10
8	99.75	96.15	100.00	98.04	99.86	97.92
9	99.62	96.23	98.08	97.14	98.90	96.94
10	99.87	100.00	98.08	99.03	99.04	98.97
11	99.75	96.15	100.00	98.04	99.86	97.92
12	99.36	100.00	90.91	95.24	95.45	95.02
13	98.60	100.00	81.03	89.52	90.52	89.35
14	99.87	100.00	97.96	98.97	98.98	98.91
15	99.87	98.08	100.00	99.03	99.93	98.97
<b>Average</b>	<b>99.61</b>	<b>97.14</b>	<b>97.22</b>	<b>97.07</b>	<b>98.51</b>	<b>96.92</b>

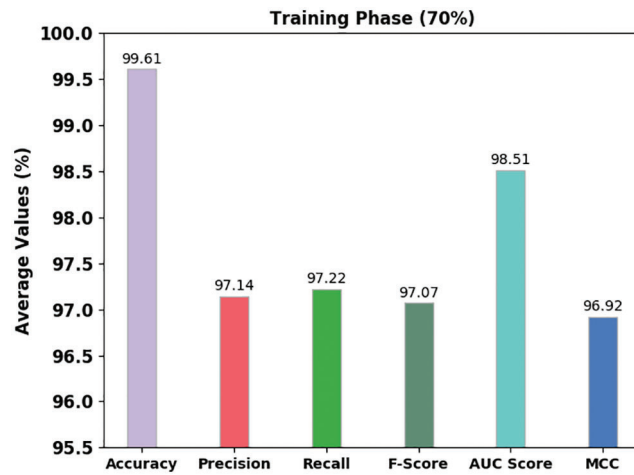


**Figure 5:** Result analysis of AMO-SCNNFC approach under 70% of TR data

Table 4 and Fig. 6 portrayed the fruit classification results of the AMO-SCNNFC technique on 30% of testing (TS) data. The AMO-SCNNFC approach has classified samples under class 1 with  $accu_y$ ,  $prec_n$ ,  $reca_l$ ,  $F_{score}$ ,  $AUC_{score}$ , and MCC of 99.70%, 100%, 96.55%, 98.25%, 98.28%, and 98.10% correspondingly. In the meantime, the AMO-SCNNFC model has categorized samples under class 5 with  $accu_y$ ,  $prec_n$ ,  $reca_l$ ,  $F_{score}$ ,  $AUC_{score}$ , and MCC of 99.70%, 96.30%, 100%, 98.11%, 99.84%, and 97.97% correspondingly. Eventually, the AMO-SCNNFC approach categorized samples under class 10 with  $accu_y$ ,  $prec_n$ ,  $reca_l$ ,  $F_{score}$ ,  $AUC_{score}$ , and MCC of 100%, 100%, 100%, 100%, 100%, and 100% correspondingly. Finally, the AMO-SCNNFC model has categorized samples under class 15 with  $accu_y$ ,  $prec_n$ ,  $reca_l$ ,  $F_{score}$ ,  $AUC_{score}$ , and MCC of 100%, 100%, 100%, 100%, 100%, and 100% correspondingly.

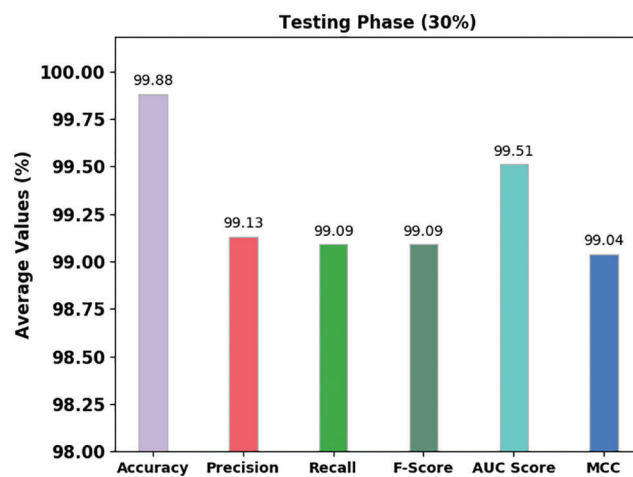
**Table 4:** Result analysis of AMO-SCNNFC approach with distinct class labels under 30% of TS data

Testing phase (30%)						
Labels	Accuracy	Precision	Recall	F-score	AUC score	MCC
1	99.70	100.00	96.55	98.25	98.28	98.10
2	100.00	100.00	100.00	100.00	100.00	100.00
3	99.70	95.00	100.00	97.44	99.84	97.32
4	100.00	100.00	100.00	100.00	100.00	100.00
5	99.70	96.30	100.00	98.11	99.84	97.97
6	100.00	100.00	100.00	100.00	100.00	100.00
7	100.00	100.00	100.00	100.00	100.00	100.00
8	100.00	100.00	100.00	100.00	100.00	100.00
9	99.41	95.65	95.65	95.65	97.67	95.33
10	100.00	100.00	100.00	100.00	100.00	100.00
11	100.00	100.00	100.00	100.00	100.00	100.00
12	100.00	100.00	100.00	100.00	100.00	100.00

(Continued)

**Table 4 (continued)**

Testing phase (30%)						
Labels	Accuracy	Precision	Recall	F-score	AUC score	MCC
13	99.70	100.00	94.12	96.97	97.06	96.86
14	100.00	100.00	100.00	100.00	100.00	100.00
15	100.00	100.00	100.00	100.00	100.00	100.00
<b>Average</b>	<b>99.88</b>	<b>99.13</b>	<b>99.09</b>	<b>99.09</b>	<b>99.51</b>	<b>99.04</b>

**Figure 6:** Result analysis of AMO-SCNNFC approach under 30% of TS data

The training accuracy (TRA) and validation accuracy (VLA) acquired by the AMO-SCNNFC method on the test dataset is shown in Fig. 7. The experimental result implicit the AMO-SCNNFC method has gained maximal values of TRA and VLA. Seemingly the VLA is greater than TRA.

The training loss (TRL) and validation loss (VLL) attained by the AMO-SCNNFC method on the test dataset were exhibited in Fig. 8. The experimental outcome denoted the AMO-SCNNFC algorithm has established the least values of TRL and VLL. Specifically, the VLL is lesser than TRL.

A clear precision-recall analysis of the AMO-SCNNFC method on the test dataset is shown in Fig. 9. The figure demonstrated that the AMO-SCNNFC method has resulted in enhanced values of precision-recall values under all classes.

A brief ROC study of the AMO-SCNNFC method on the test dataset is exhibited in Fig. 10. The results denoted the AMO-SCNNFC method has shown its ability in categorizing distinct classes on the test dataset.

Table 5 highlights an overall comparison study of the AMO-SCNNFC model with existing techniques [22]. Fig. 11 demonstrates the comparative  $accu_y$  inspection of the AMO-SCNNFC with other methodologies. The figure implied that the MobileNetV1 and Inception v3 techniques had exhibited poor outcomes with minimal  $accu_y$  of 86.58% and 90.35% respectively. Next, the DenseNet121, VGG-16, and MobileNetV2 models have shown closer  $accu_y$  of 94.94%, 95.24%, and 96.21% respectively. Though the

AFC-HPODTL model has reported considerable *accu<sub>y</sub>* of 99.48%, the AMO-SCNNFC model has shown enhanced outcomes with maximum *accu<sub>y</sub>* of 99.88%.

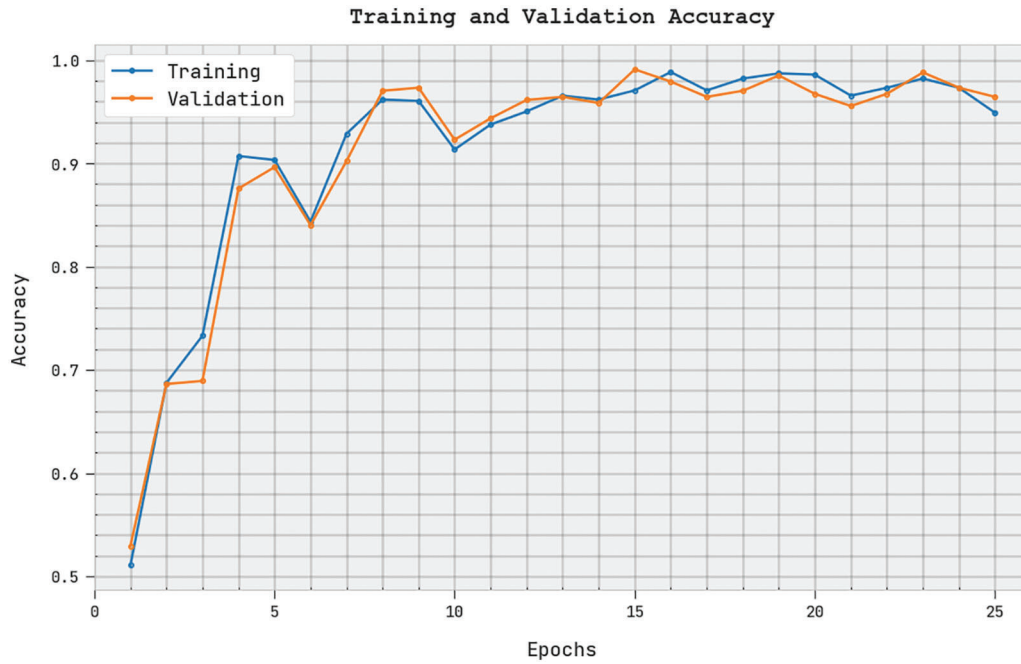


**Figure 7:** TRA and VLA analysis of AMO-SCNNFC methodology



**Figure 8:** TRL and VLL analysis of AMO-SCNNFC methodology

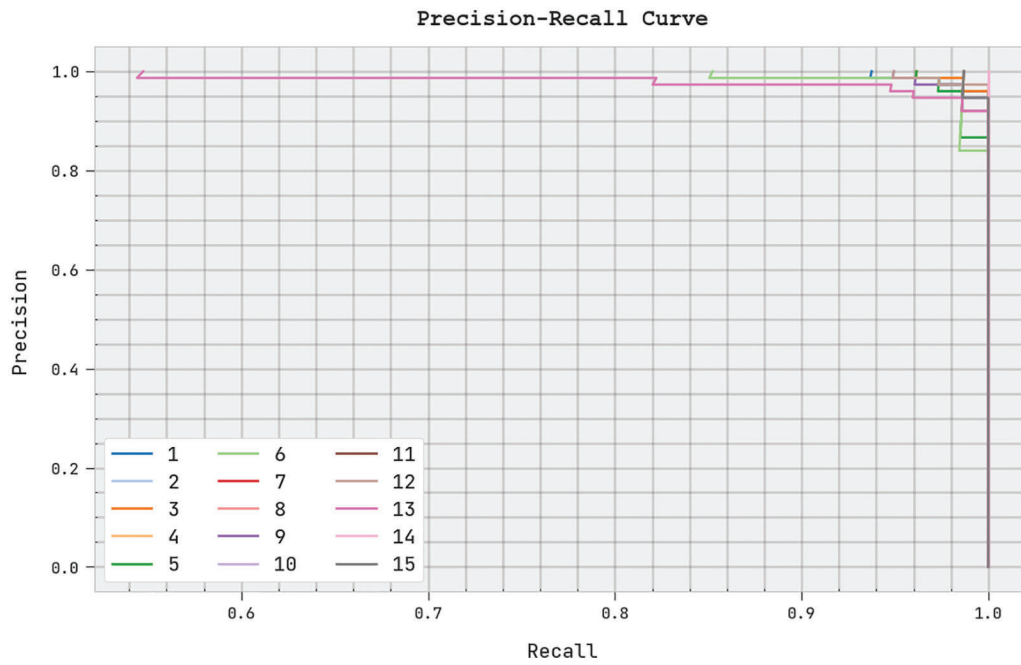


**Figure 9:** Precision-recall analysis of AMO-SCNNFC methodology

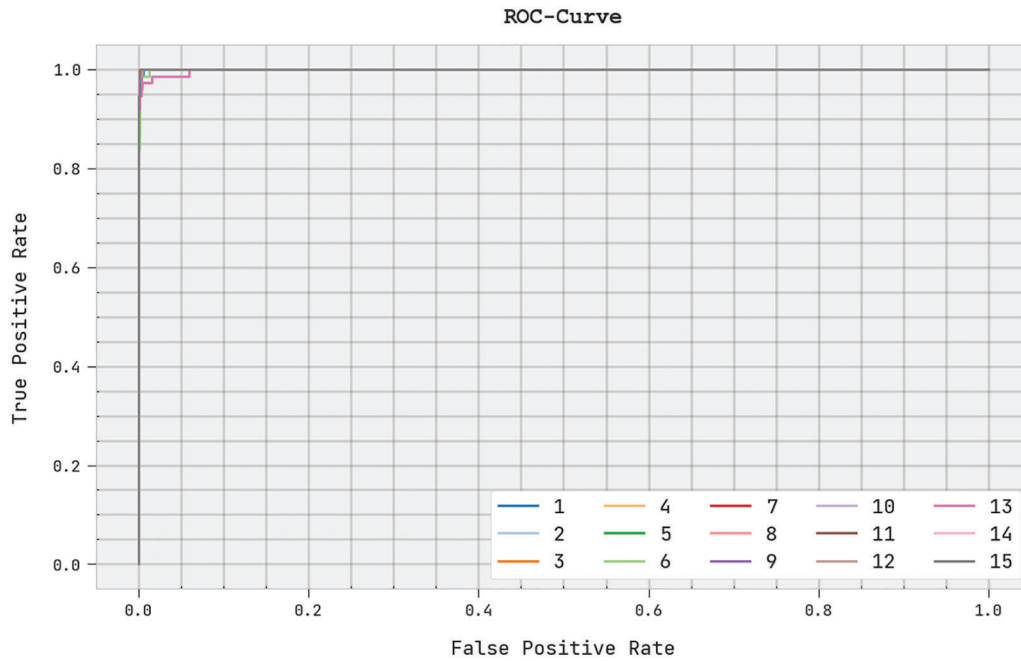


**Figure 10:** ROC analysis of AMO-SCNNFC methodology

**Table 5:** Comparative analysis of AMO-SCNNFC approach with existing approaches

Methods	Accuracy	Precision	Recall	F1-score
DenseNet121 model	94.94	93.86	94.95	94.48
VGG-16 model	95.24	94.41	94.24	94.12
MobileNetV1 model	86.58	87.76	86.23	86.02
InceptionV3 model	90.35	90.40	89.06	89.10
MobileNetV2 model	96.21	95.24	95.58	95.84
AFC-HPODTL model	99.48	98.80	99.03	98.43
AMO-SCNNFC	99.88	99.13	99.09	99.09

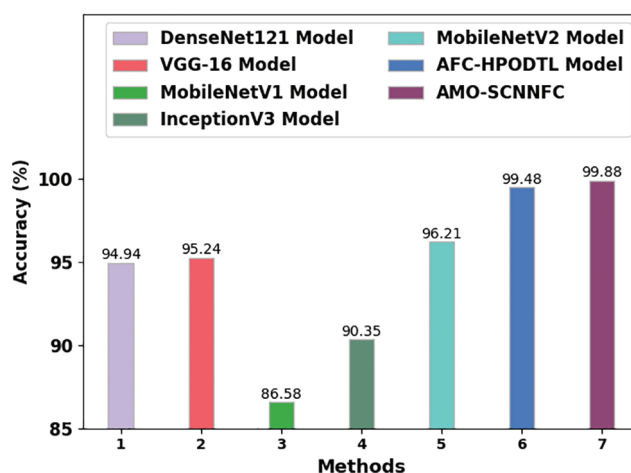
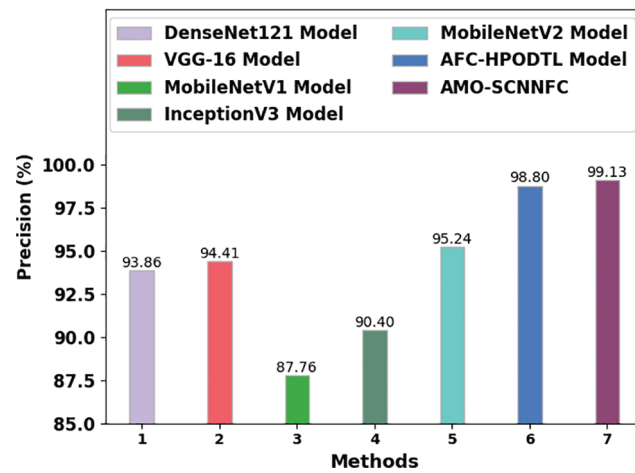
**Figure 11:**  $Accu_y$  analysis of the AMO-SCNNFC approach with existing methodologies

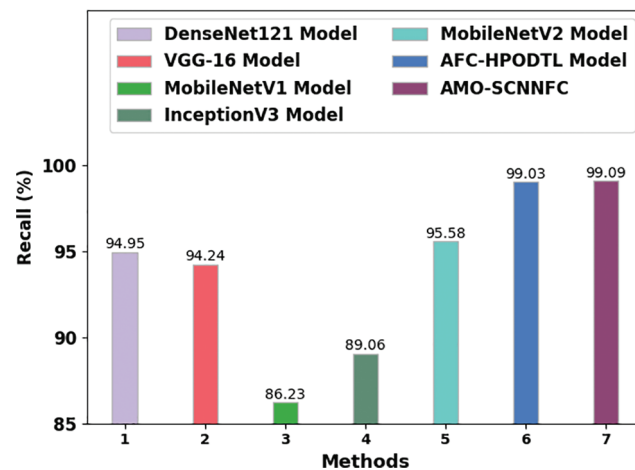
Fig. 12 establishes the comparative  $prec_n$  scrutiny of the AMO-SCNNFC algorithm with other models. The figure implied that the MobileNetV1 and Inception v3 models have shown poor outcomes with minimal  $prec_n$  of 87.76% and 90.40% correspondingly. Then, the DenseNet121, VGG-16, and MobileNetV2 models have shown closer  $prec_n$  of 93.86%, 94.41%, and 95.24% correspondingly. Though the AFC-HPODTL approach has reported considerable  $accu_y$  of 98.80%, the AMO-SCNNFC technique has shown enhanced outcomes with maximum  $prec_n$  of 99.13%.

Fig. 13 validates the comparative  $reca_l$  investigation of the AMO-SCNNFC with other models. Even though the AFC-HPODTL model has reported considerable  $accu_y$  of 99.03%, the AMO-SCNNFC approach has shown enhanced outcomes with maximal  $reca_l$  of 99.09%.

The results implied that the MobileNetV1 and Inception v3 models have displayed shown poor outcomes with minimal  $F_{score}$  of 86.02% and 89.10% respectively. Though the AFC-HPODTL method has reported considerable  $accu_y$  of 98.43%, the AMO-SCNNFC algorithm has shown enhanced outcomes with maximum  $F_{score}$  of 99.09%. Thus, the AMO-SCNNFC model can be considered an accurate fruit classification model.



**Figure 12:**  $Prec_n$  analysis of the AMO-SCNNFC approach with existing methodologies



**Figure 13:**  $Reca_l$  analysis of the AMO-SCNNFC approach with existing methodologies

#### 4 Conclusion

In this study, a new AMO-SCNNFC model has been developed for the automated classification of fruits. The presented AMO-SCNNFC technique encompasses preprocessing, VGG-16 feature extraction, SPO hyperparameter tuning, ESCNN classification, and AHO-based parameter optimization. The utilization of SPO and AHO techniques helps in accomplishing enhanced fruit classification performance. For fruit classification, AHO with the SCNN model is applied to identify different classes of fruits. The performance validation of the AMO-SCNNFC technique is tested using a dataset comprising diverse classes of fruit images. Extensive comparison studies reported the betterment of the AMO-SCNNFC technique over other approaches with higher accuracy of 99.88%. Thus, the AMO-SCNNFC technique can be utilized for the effectual fruit classification process. In the future, three DL-based fusion approaches can be developed to improve detection performance.

**Funding Statement:** This work was supported by Basic Science Research Program through the National Research Foundation of Korea (NRF) funded by the Ministry of Education (2020R1A6A1A03038540) and by Korea Institute of Planning and Evaluation for Technology in Food, Agriculture, Forestry and Fisheries (IPET) through Digital Breeding Transformation Technology Development Program, funded by Ministry of Agriculture, Food and Rural Affairs (MAFRA) (322063-03-1-SB010) and by the Technology development Program (RS-2022-00156456) funded by the Ministry of SMEs and Startups (MSS, Korea).

**Conflicts of Interest:** The authors declare that they have no conflicts of interest to report regarding the present study.

## References

- [1] J. N. Torres, M. Mora, R. H. García, R. J. Barrientos, C. Fredes *et al.*, “A review of convolutional neural network applied to fruit image processing,” *Applied Sciences*, vol. 10, no. 10, pp. 3443, 2020.
- [2] D. Shakya, “Analysis of artificial intelligence based image classification techniques,” *Journal of Innovative Image Processing (JIIP)*, vol. 2, no. 1, pp. 44–54, 2020.
- [3] M. Tripathi, “Analysis of convolutional neural network based image classification techniques,” *Journal of Innovative Image Processing (JIIP)*, vol. 3, no. 2, pp. 100–117, 2021.
- [4] D. T. P. Chung and D. V. Tai, “A fruits recognition system based on a modern deep learning technique,” *Journal of Physics: Conference Series*, vol. 1, pp. 012050, 2019.
- [5] R. G. de Luna, E. P. Dadios, A. A. Bandala and R. R. P. Vicerra, “Size classification of tomato fruit using thresholding, machine learning, and deep learning techniques,” *AGRIVITA, Journal of Agricultural Science*, vol. 41, no. 3, pp. 586–596, 2019.
- [6] F. Valentino, T. W. Cenggoro and B. Pardamean, “A design of deep learning experimentation for fruit freshness detection,” *IOP Conference Series: Earth and Environmental Science*, vol. 794, no. 1, pp. 012110, 2021.
- [7] M. Bayğın, “Vegetable and fruit image classification with squeezeNet based deep feature generator,” *Turkish Journal of Science and Technology*, 2022. <https://dx.doi.org/10.55525/tjst.1071338>
- [8] V. A. Meshram, K. Patil and S. D. Ramteke, “MNet: A framework to reduce fruit image misclassification,” *Ingénierie des Systèmes d’Information*, vol. 26, no. 2, pp. 159–170, 2021.
- [9] F. Risdin, P. K. Mondal and K. M. Hassan, “Convolutional neural networks (CNN) for detecting fruit information using machine learning techniques,” *IOSR Journal of Computer Engineering (IOSR-JCE)*, vol. 22, no. 2, pp. 1–13, 2020.
- [10] M. Hossain, M. Al-Hammadi and G. Muhammad, “Automatic fruit classification using deep learning for industrial applications,” *IEEE Transactions on Industrial Informatics*, vol. 15, no. 2, pp. 1027–1034, 2019.
- [11] X. Chen, G. Zhou, A. Chen, L. Pu and W. Chen, “The fruit classification algorithm based on the multi-optimization convolutional neural network,” *Multimedia Tools and Applications*, vol. 80, no. 7, pp. 11313–11330, 2021.
- [12] S. Ashraf, I. Kadery, M. A. A. Chowdhury, T. Z. Mahbub and R. M. Rahman, “Fruit image classification using convolutional neural networks,” *International Journal of Software Innovation*, vol. 7, no. 4, pp. 51–70, 2019.
- [13] H. S. Gill and B. S. Khehra, “Hybrid classifier model for fruit classification,” *Multimedia Tools and Applications*, vol. 80, no. 18, pp. 27495–27530, 2021.
- [14] T. B. Shahi, C. Sitaula, A. Neupane and W. Guo, “Fruit classification using attention-based MobileNetV2 for industrial applications,” *PLoS One*, vol. 17, no. 2, pp. e0264586, 2022.
- [15] L. Zhu, Z. Li, C. Li, J. Wu and J. Yue, “High performance vegetable classification from images based on AlexNet deep learning model,” *International Journal of Agricultural and Biological Engineering*, vol. 11, no. 4, pp. 213–217, 2018.
- [16] Y. D. Zhang, Z. Dong, X. Chen, W. Jia, S. Du *et al.*, “Image based fruit category classification by 13-layer deep convolutional neural network and data augmentation,” *Multimedia Tools and Applications*, vol. 78, no. 3, pp. 3613–3632, 2019.

- [17] S. Srivastava, P. Kumar, V. Chaudhry and A. Singh, "Detection of ovarian cyst in ultrasound images using fine-tuned vgg-16 deep learning network," *SN Computer Science*, vol. 1, no. 2, pp. 81, 2020.
- [18] A. Kaveh and S. Mahjoubi, "Hypotrochoid spiral optimization approach for sizing and layout optimization of truss structures with multiple frequency constraints," *Engineering with Computers*, vol. 35, no. 4, pp. 1443–1462, 2019.
- [19] M. H. Ali, M. M. Jaber, S. K. Abd, A. Rehman, M. J. Awan *et al.*, "Threat analysis and distributed denial of service (ddos) attack recognition in the internet of things (IoT)," *Electronics*, vol. 11, no. 3, pp. 494, 2022.
- [20] A. Ramadan, S. Kamel, M. Hassan, E. Ahmed and H. Hasaniien, "Accurate photovoltaic models based on an adaptive opposition artificial hummingbird algorithm," *Electronics*, vol. 11, no. 3, pp. 318, 2022.
- [21] A. Rocha, D. Hauagge, J. Wainer and S. Goldenstein, "Automatic fruit and vegetable classification from images," *Computers and Electronics in Agriculture*, vol. 70, no. 1, pp. 96–104, 2010.
- [22] K. Shankar, S. Kumar, A. K. Dutta, A. Alkhayyat, A. J. M. Jawad *et al.*, "An automated hyperparameter tuning recurrent neural network model for fruit classification," *Mathematics*, vol. 10, no. 13, pp. 2358, 2022.